Structural Analysis of Historical Constructions, New Delhi 2006
P.B. Lourenço, P. Roca, C. Modena, S. Agrawal (Eds.)

Testing for Assessment of Load Carrying Capacity of Masonry Arch Bridges

Kumar Pardeep
Civil engineering Department, National Institute of Technology Hamirpur,(HP), India -177005

N.M. Bhandari
Professor, Department of Civil Engineering, Indian Institute of Technology Roorkee (UA), India - 247667

ABSTRACT: A significant number of masonry arch bridges in India, constructed in the pre-independence era are carrying vehicles with axle loads and speeds far beyond their design load. The tests have been conducted on four test arches with 2.53 m span, 0.70 m rise, and 0.717 m width with two rings of bricks. Two of these were vault only arches and other two had spandrel walls and fill also. Each of the arches had two half brick thick rings. The arches were loaded at the quarter point till the formation of hinges at four locations leading to a mechanism failure. Although similar tests have been carried out previously by many researchers, the properties of the masonry are influenced by its constituents so for the type of bricks available in India, it was deemed necessary to conduct a series of the tests. The paper presents the results of tests conducted on the arches in the laboratory to determine the load carrying capacity of the arches, and to understand its behaviour till failure. The testing was carried out for the validation of non-linear finite element analysis program using the experimentally developed constitutive relation for masonry. The location of the hinge formation differed in the two identical arches, indicating the non-repeatability and uncertainty associated with the behaviour and the collapse load. The paper also addresses issues regarding the strengthening techniques employed for the masonry arch bridges.

1 INTRODUCTION

In recent years, a considerable amount of effort has gone into research concerning the load carrying capacity of masonry arch bridges. The reason for this upsurge in interest can be largely attributed to the increase in the traffic volume and higher axle loads. The design details of large number of such bridges are not known yet these are catering to present day functional requirements. These are able to carry such high loads due to the inherent strength of the structural arch form and considerable factors of safety by way of conservative values for stresses in the materials used at the time of the design. However, most of the arch bridges are overstressed and show various signs of distress due to increased loads and material deterioration. The studies substantiated by full scale testing programs on abandoned masonry arch bridges and model testing has helped bridge engineers to better understand their behavior and make a reasonable estimate of the load carrying capacity of these bridges.

The Literature contains numerous reports on the experimental study of arch behavior using model structures. Heyman (1982) summarized reports of tests conducted on the voussoir arches. The work done by Pippard et al. (1951) clarified the mechanics of the voussoir arches and formation of the successive hinges leading to a mechanism failure. Later Royles and Hendry (1991) conducted tests on 24 model arch bridges of variable span and span to depth ratio, to establish the effect on strength of arch due to presence of fill, spandrel and wing walls. Melbourne et al. (1988) conducted similar tests on masonry arches. Ng et al. (1999) conducted tests on three large-scale soil backfilled arch bridges to investigate the repeatability of ultimate load and

collapse mechanism and concluded that identical arches may yield significantly different collapse loads. Hogg and Choo (2000) conducted tests on a series of eight models to destruction to study the scaling effects for the use of small-scale models to predict the capacity of the large-scale structures.

In the following paper, the results of an experimental investigation conducted study the behavior of masonry arches and to determine their load carrying capacity have been presented. The program included constructing four arches, two each of similar geometry and subjecting them to static monotonically increasing loads up to failure. The first set consisted of the arch barrel and the second set consisted of arch barrel with spandrel walls and overlaying fill. The geometric data of the test arches constructed is given in Table 1.

Table 1.: Dimensions of the test arches.

Arch	Span (m)	Rise (m)	Thickness (m)	Width (m)	Height of spandrels over crown (m)	Thickness of spandrel walls (m)	Geometry
AV1 & AV2	2.53	0.70	0.236	0.717	-	-	Segmental
AF1 & AF2	2.53	0.70	0.236	0.717	0.20	0.115	Segmental

2 EXPERIMENTAL INVESTIGATION

The experimental investigation was carried out to determine the load carrying capacity and to understand the behavior of the masonry arches constructed using indigenous materials. Further, the experimental investigation was carried out for the validation of the finite element program developed for the analysis of masonry arches (Kumar 2005). The arches were constructed using the full-scale table-molded bricks from local kiln in Roorkee. The details of the arches are shown in Fig. 1 and Fig. 2 respectively. The bricks were laid in 1:4 cement sand mortar. The arch models were constructed on the fabricated foundation with inclined springing on the transverse girders of the loading frame.

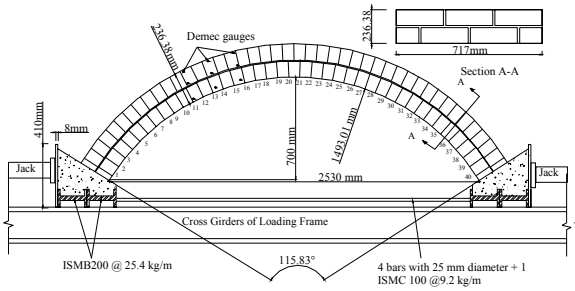

Figure 1 : Details of Arches AV1 and AV2.

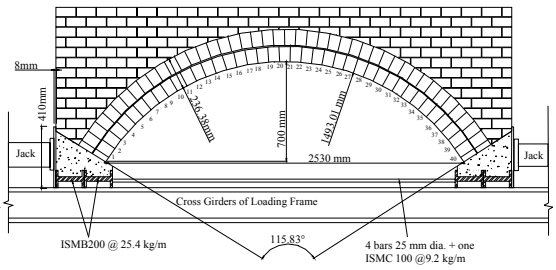

Figure 2 : Details of Arches AF1 and AF2

2.1 Foundation

Two sets of abutments were fabricated using steel sections, such that two arch models could be constructed at the same time. The distance between the inner edges of the abutments was kept as 2420 mm. The abutments were constructed on two-rolled steel I-beam sections ISMB 200@ 25.4 kg/m) welded to each other longitudinally along the flanges. These were connected with help of tie rods (4 – 25 mm) and a channel sections (ICMS 100@ 9.2 kg/m) sufficient to resist the horizontal thrust at the time of collapse. This grid was adequately tied to the cross girders of the frame so that horizontal, and vertical reactions and moment could develop at the springing. The concrete cast on the end sections provided an angle embrace of 115.83º and a rise of 0.7 m.

2.2 Material and their properties

The table moulded brick having average size of 227 mm × 108 mm × 73 mm, water absorption as per IS 3495 (Part II)-1992 as 11.42 %, average compressive strength of 19.11 N/mm^2 with a standard deviation of 3.45 N/mm^2 have been used. Ordinary Portland Cement of Grade 53 as per IS 12269-1989, having 28 day compressive strength as 60.96 N/mm^2 was used in the preparation of 1:4 cement sand mortar with river washed sand from nearby river. The water cement ratio of 0.35 was used for the construction of control specimens and was left to the discretion of the mason for the construction of the arches. The fineness modulus of sand used was 1.87. The tests were conducted on the masonry prisms and pillars to investigate the properties of masonry as shown in Table 2.

Table 2 : Properties of the materials.

Bricks

Average Dimension (mm)				Water Absorption (%)	Efflorescence	Comp. Strength (MPa)	Modulus at 25% of Ultimate Strain	Poisson Ratio	Ultimate Strain
	Length	Width	Height						
Average	227.85	108.85	73.01	11.42	Nil	19.11	4822.70	0.144	0.378
S. D.	3.66	2.23	1.18	1.26	Nil	3.45	559.58	0.11	0.023

1:4 Cement Sand Mortar

Cement					Sand	W/C	Mortar			
	IST (min)	FST (min)	7-Day Comp. Strength (MPa)	28-Day Comp. Strength (MPa)	Fineness Modulus	% flow	Comp. Strength (MPa)	Modulus at 25% of Ultimate Strain	Poisson Ratio	Ultimate Strain
Average	100	220	34.55	60.96	1.87	110-115	14.817	12164.01	0.172	0.267
S. D.	-	-	-	-	-	-	0.806	1425.07	0.009	0.049

Masonry

	Average Dimension (mm)			Comp. Strength (MPa)	Comp. Strain (%)	Modulus at 25% of Ultimate Strain	Poisson Ratio	Tensile Strength (MPa)	Bond Shear Strength (MPa)	Coeff. of Friction
	Length	Width	Height							
Prism P1	222.81	105.13	416.21	5.841	0.315	3723.03	0.17	-	-	-
Pillar P2	229.81	229.86	493.79	5.059	0.4132	2180.05	0.175	-	-	-
Prisms	681	105	223	-	-	-	-	0.29	-	-
Couplets	223	105	156	-	-	-	-	-	0.358	0.874

2.3 Method of Construction

The arches had two rings separated with a mortar joint of 12 mm. The two rings together represented a thickness of one brick i.e. 236.38 mm. The joint thickness was kept uniform throughout the circumference of the arch. The bricks were laid in header bond across the width as seen in the Fig. 3. The arches consisted of 39 bricks in the inner layer and 42 bricks in outer layer through the circumference, 3 bricks across the width, which was equivalent to 717 mm.

The first layer of the bricks was laid over the formwork starting from one abutment up to the quarter point of the arch. Subsequently starting from the second abutment the first layer was laid up to the quarter point. Thereafter following the same procedure the remaining courses were laid simultaneously from both the ends such that the joint thickness could be attuned to adjust the full brick at the crown. The procedure was then repeated for the second layer of the bricks. The verticality of the joints was staggered by the use of the brickbats in the alternate courses, in order to avoid the direct planes of weakness and minimize the possibility of shear failure. The arches were then covered with wet gunny bags in order to prevent premature hydration and were allowed to cure for 28 days

The backfill consisting of coarse sand was filled over the vault confined by the spandrel walls. The backfill was filled in the model by the Rainfall method to achieve a density of 1.889 gm/cm^3. The fill was dropped uniformly from a height of 60 cm to obtain this density through out. The depth of the fill over the crown was kept as 200 mm. The backfill moisture content was 12 %. The backfill material was subjected to a series of unconsolidated undrained direct shear tests under different normal loads to determine the apparent cohesion and the angle of shearing resistance. The samples were compacted to a bulk unit weight of 18.89 kN/m^3 and the test was performed under the unsaturated conditions. The apparent cohesion of the backfill was determined to be 0 and its angle of shearing resistance was found to be 59.56º. The average particle size distribution of the backfill material when dry sieved is given in Table 3. and its fineness modulus was 3.40.

Table 3 : Average particle size distribution of backfill material.

I. S. Sieve No.	Weight Retained (gm)	% Weight Retained	Passing	Cumulative Retained
480	105	21	79	21
240	65	13	60	34
120	80	16	50	50
60	35	7	43	57
30	120	24	19	81
15	80	16	3	97
Pan	15	3	0	100
	∑ = 500	Fineness Modulus = 3.40		

3 INSTRUMENTATION FOR MEASUREMENTS

3.1 Displacements

Proving ring of 200 kN with a least count of 1.635 kN was used for the measurement of the applied load on the arch. To measure the deflections in the radial direction, the dial gauges having least count of 0.01 mm were positioned at the crown, quarter points, and near the abutments on the intrados of arch. The gauges were mounted over an independent platform fabricated of rolled steel angle sections (Fig. 4). This was done to avoid the interference of the deflections induced in the supporting girders of the loading frame. Over each section three dial gauges were mounted, two over the end and one in the center of the barrel to check that the arch was deflecting uniformly across the width. The dial gauges were positioned over the 25 mm × 25 mm brass plates glued to the surface of the brickwork. For second set of the models, LVDT's were placed along the centerline of the arch at two-quarter points and under the crown.

3.2 Strains

The strain distribution through the depth of arch barrel was measured using a demec gauge with sets of demec points. These sets of demec points were positioned through the rib thickness at four locations on either side of the arch. The demec points consisted of brass studs having 10 mm diameter and 10 mm height, glued to the surface of the arch barrel face by instant hardening glue. The demec points were positioned at the potential crack locations in the arch rib, which were expected to exhibit the maximum variation in the strains. However, over the quarter point opposite to the load point these demec points spread over larger range, as the potential crack location over this location varies with the increase in the applied load.

3.3 Loads

The arches were loaded one by one at quarter point through a 200 kN hydraulic jack packed between the arch and transverse beam of the reaction frame. In order to simulate the live load distributed uniformly across the width of the arch, the line load was applied through sufficiently high built up I - beam section resting over an appropriate seating made in plain cement concrete (1:1.5:3) on the brickwork of the arch barrel extending over the full width of the beam. In order to ensure the uniformity of loading throughout the width of the arch, the spreader beam was

centrally placed under loading jack. The spreader beam was bedded on lean cement sand mortar to ensure that the bearing was perfect and it is horizontal.

It was appreciated that by casting this step on the arch barrel, the arch would be stiffened, but as only one step was cast the stiffening was localized over the smaller portion of the arch barrel. The stiffening effect indeed must not have significantly contributed to the overall strength of the arch barrel, but certainly increased the dispersion width of the load under the spreader beam to the arch barrel. The dead load due to the fill and the spandrel walls was absent for the vault only models, as the aim was to explicitly determine the load carrying capacity of the arch barrel. The loading was applied manually in small increments.

Figure 3 : Construction of arch barrel in progress.

Figure 4 : Placement of dial gauges and LVDT's.

4 TESTING OF ARCHES

Initially the arches were loaded to a load of 20 kN and then the load was removed. This was done several times in order to check for any false deflection due to the presence of any voids /looseness or cavities. Testing of the arches to collapse was conducted by incrementing the hydraulic pressure in the pump attached to the hydraulic jack. The loading was applied manually in small increments of 2.5 kN. The loading was maintained over the test arch at every increment for duration of about 5 minutes before taking down the reading. It was observed that the readings of the dial gauges used for the measurement of the deflections stabilized within 5 minutes.

5 EXPERIMENTAL RESULTS

The experimental results of testing of arch models given under. Every load increment followed the visual inspection of the arch for the onset of cracking. The summary of the failure load and the locations of the hinges are given in Table 4. The vertical joints in the two layers of the arch vault were staggered. The results are reported with respect to the joint numbers of the layer on the intrados. The sequence of hinge formation is also reported in Table 4.

5.1 Behavior of arch AV1

A uniformly distributed line load across the full width was applied to the arch at quarter span. The arch did not collapse, but failed due to the formation of the four hinges at the joints near the abutments and quarter points. The arch was loaded in increments of 2.5 kN upto a load of 54.18 kN, at which the arch cracked simultaneously under the point load and left quarter point. The load suddenly dropped to 43.39 kN and the corresponding displacements increased, due to the loss of the stiffness and the widening of cracks took place. The load was again increased in even smaller increments up to 45.35 kN at which the arch cracked at the third location near the left abutment (Far from load point), and load again fell to 43.39 kN. At this instant the dial gauges were removed and the load was further increased, the load did not go beyond the last load level but another hinge was formed near the right abutment and the cracks further widened

up. No signs of the compressive failure of arch material were observed. The arch failed due to conversion to a mechanism after the formation of the hinges at four locations as seen in Fig. 5.

5.2 Behavior of arch AV2

This arch was also loaded in increments of 2.5 kN up to a load of 49.05 kN, at which the arch cracked simultaneously under the point load and left quarter point. The load suddenly dropped to 34.34 kN and there was sudden increase in the displacements. The load was again increased in even smaller increments up to 39.34 kN at which the arch cracked at the third location near the left abutment (Far from load point), and load again fell to 37.87 kN. At this instant the dial gauges were removed and the load was further increased. Another hinge formed near the right abutment and the cracks further widened up. No signs of the compressive failure of arch material were observed. This arch also failed due to formation of mechanism after the formation of hinges at the identical four locations as seen in Fig. 6.

Table 3 : Failure loads and the hinge locations.

Arch	First Crack Load	Failure Load (kN)	Sequence of Hinge Formation	Hinge Location (Mortar joint numbers from left)	Face
AV1	54.18	56.14	1st and 2nd concurrently	25 and 14	1st on Extrados & 2nd on Intrados
			3rd	2	Extrados
			4th	40	Intrados
AV2	49.05	54.05	1st and 2nd concurrently	30 and 12	1st on Extrados & 2nd on Intrados
			3rd	2	Extrados
			4th	40	Intrados
AF1	40.00	73.00	1st	27	Extrados
			2nd	8	Intrados
			3rd	17	Intrados
			4th	38	Intrados
AF2	42.50	75.50	1st	26	Extrados
			2nd	10	Intrados
			3rd	14	Intrados
			4th	37	Intrados

5.3 Behavior of arch AF1

The arch model AF1 was filled up with the coarse sand. The live load, uniformly distributed through the surface of the backfill, over an area of 340 mm × 400 mm was applied in increments of 2.5 kN. Up to a load of 40 kN no distress or cracking was observed in any part of the arch. Just in next increment a crack was observed under the point load on the intrados of the arch. Subsequently upon, further increase in load, the crack extended along the extrados of the arch, leading to the separation of the spandrel wall from the barrel. This crack extended towards the crown as well as towards the right abutment as shown in Fig. 7. At a load of 60 kN, spandrel wall cracked above left abutment and further increase in the load lead to the cracking of spandrel in vertical direction under the load point as seen in Fig. 7. At a load level of 73 kN a crack formed near the crown and also near the right abutment. At this instant the LVDTs and Dial gauges were removed and arch did not take any further load.

Figure 5 : Cracks developed near left abutment, left quarter point and crown for arch AV1.

Figure 6 : Cracks developed near left abutment, left quarter point and crown for arch AV2.

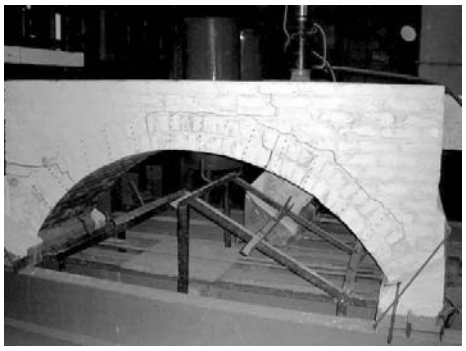

Figure 7 : Cracks in the arch barrel and the spandrel wall in AF1 arch.

Figure 8 : Cracks in the arch barrel and the spandrel wall in AF2 arch.

5.4 Behavior of arch AF2

The arch was loaded at right quarter span. The load deflection behaviour of arch AF2 was observed almost similar to AF1. The first visible crack occurring under the load in the arch was observed at 42.5 kN. The crack led to initiation of separation of spandrel wall from the arch barrel progressing towards crown as well as right abutment. When load reached 67.5 kN another crack splitting the spandrel wall over the left abutment appeared and led in to arch barrel (Fig. 8). With further increase in the load these cracks kept on opening. A crack in the vicinity of this crack appeared on the extrados that led up to the top of spandrel wall when the load was raised to 74.8 kN. In the meantime, the crack propagating towards right abutment also entered the barrel when load was being raised to 75.5 kN. Finally the load dropped to 73.2 kN. Further application of load merely increased the deflections and load levels did not increase.

6 LOAD DEFLECTION BEHAVIOUR

The load deflection plots for arches are presented in Fig. 9 and Fig. 10. It can be readily observed that after the formation of the crack under the load point and left quarter point almost simultaneously, the stiffness of the structure in these regions reduced significantly. The deflections observed at this instant include the adjustments of the arch profile on account of insertion of two hinges. This simultaneously followed a drop in the load observed. Although the failure of the arch sections was due to material tensile failure, but the final failure of the arch as a whole took the form of the mechanism.

For the arches the load deflection is almost linear up to the formation of the first hinge or crack. The deflections after this load level increased because these include the rigid body movements due to the adjustment of the thrust line within the arch barrel.

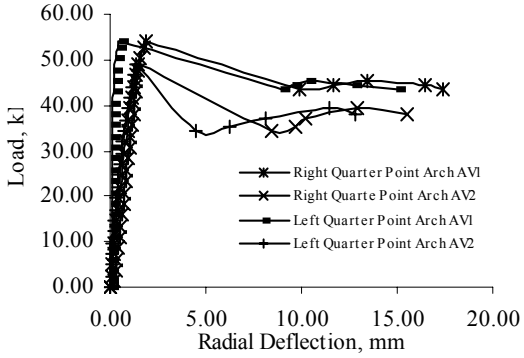

Figure 9 : Load deflection plot for Arches AV1 and AV2 under load point and left quarter point.

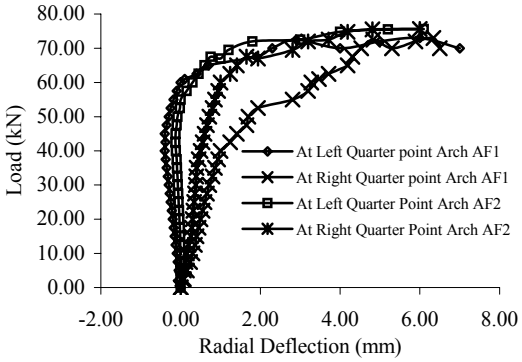

Figure 10 : Load deflection plots for arches AF1 and AF2 under load point and left quarter point..

7 CONCLUSIONS

The arches although had similar geometry, material as well as workmanship, failed at nearly same loads. The arches failed as mechanism, due to formation of hinges primarily at four significant locations. The first hinge developed under the load point and the second at the opposite quarter point. The third and fourth hinges formed subsequently near the abutments.

The load deflection plots are linear up to formation of the first hinge. Due to sudden release of tension energy due to tensile cracking, arch looses its stiffness as can be seen from load deflection curves.

It is seen that a substantial part of the maximum load carrying capacity of an arch is resisted prior to the formation of the first hinge. The additional load required for the formation of the remaining three hinges is very small. This observation is based on experimental observation.

The compressive failure as well as the shear failure of masonry had not been observed anywhere in the arch. May be the self-weight thrust in the test arches were very low.

The material compressive failure was not observed anywhere in the arch.

The spandrel walls and the fill contribute substantially to the stiffness as well as load carrying capacity of the arches.

REFERENCES

Heyman, J., 1982, *The Masonry Arch* (Ellis Horwood, Chichester)

Hogg, V. and Choo, B. S., 2000, *A Study of Scale Effects in Masonry Arch Bridges: Is Testing of Large Scale Structures Still Necessary?* The Structural Engineer, 7, Vol. 78, No. 5, pp. 24-29.

IS 12269: 1989, Indian Standard Specification for 53 Grade Ordinary Portland Cement, Bureau of Indian Standards, New Delhi.

IS 2250: 1981, Indian Standard Code of Practice for Preparation and Use of Masonry Mortars, Bureau of Indian Standards, New Delhi.

IS 3495: 1992, (Part 1 – 4), Indian Standard Methods of Tests of Burnt Clay Building Bricks - Part 1: Determination of Compressive Strength - Part 2: Determination of Water Absorption - Part 3: Determination of Efflorescence - Part 4: Determination of Warpage, Bureau of Indian Standards, New Delhi.

Kumar, Pardeep, 2005, Load Rating and Assessment of Masonry Arch Bridges, Ph.D. Thesis, Indian Institute of Technology, Roorkee, July, 2005.

Melbourne, C. Walker, P. J., 1988, Load Tests to Collapse of Model Brickwork Masonry Arches, *Proc. 8th Int. Brick and Block Masonry Conference,* Dublin, Vol. 2, Elsevier Applied Science, New York, Pp. 991-1002

Ng, K. H. & Fairfield, C. A., 1999, Collapse Load Repeatability Tests on Brickwork Arches, Structural Faults + Repair – 99.

PIPPARD, A. J. S.; and CHITTY, L. A. 1951, *Study of the Voussior Arch*, National Building Studies Research Paper No. 11, HMSO London.

Royles, R. and Hendry, A. W., 1991, Model Tests on Masonry Arches, *Proceedings Institution of Civil Engineers, Structures and Buildings*, 91, June, Pp. 299 - 321.